0026-895X/03/6301-174–182$7.00
MOLECULAR PHARMACOLOGY
Vol. 63, No. 1
1859/1033633
Mol Pharmacol 63:174–182, 2003
Printed in U.S.A.

Structural Characteristics That Govern Binding to, and Modulation through, the Cardiac Ryanodine Receptor Nucleotide Binding Site

WEI MUN CHAN, WILLIAM WELCH, and REBECCA SITSAPESAN

University of Bristol, Department of Pharmacology, School of Medical Sciences, University Walk, Bristol, United Kingdom (W.M.C., R.S.); University of Nevada School of Medicine, Department of Biochemistry, Reno, Nevada, Nevada (W.W.)

Received May 20, 2002; accepted October 8, 2002

This article is available online at http://molpharm.aspetjournals.org

ABSTRACT

Comparative molecular field analysis (CoMFA) predicts that the large electrostatic field around the phosphate groups of ATP plays a crucial role in stabilizing the open state of the cardiac ryanodine receptor (RyR) channel. We therefore investigated the effects of adenosine-5′-(β,γ-methylenetriphosphate) (AMP-PCP), an ATP analog with lower negative charge in this region, on the gating of the cardiac RyR channel. In the presence of 10 μM cytosolic Ca^{2+}, AMP-PCP exhibited approximately 50% of the efficacy of ATP and optimal doses increased open probability (P_o) to only 0.441 $\pm$ 0.156 ($n = 4$), thus confirming the predictive ability of our preliminary CoMFA model. We also reveal that AMP-PCP has a higher affinity than ATP for the cardiac RyR, demonstrating that the structural properties required for tight binding to RyR differ from those necessary for recruiting long open states and high P_o values. CoMFA identified very strong correlations between the structures of adenine-based ligands and their affinity for RyR and different (but also highly significant) correlations between structure and the ability to activate the channel. Analysis indicates that ATP may be more effective than other adenine nucleotides because it can convert the greatest amount of binding energy into conformational changes that stabilize the open channel state.

ATP and related adenine nucleotides present in cardiac cells have an important function as regulators of RyR channel gating. ATP can induce long open events and a high open probability (P_o) in the presence of micromolar cytosolic Ca^{2+} (Kermode et al., 1998). High levels of adenine nucleotides and Ca^{2+} tend to inactivate the channel (Kermode et al., 1998; Ching et al., 1999); therefore, the effects of this group of ligands are complex and are likely to shape both the activation and inactivation processes of intracellular Ca^{2+} release in cardiac cells. Understanding the underlying molecular nature of the binding of adenine nucleotides to RyR channels and the structural features of ATP that produce open RyR channels is therefore important for a greater understanding of how RyR channels are regulated during the process of excitation-contraction coupling. In a preliminary CoMFA study, we previously correlated the structure of ATP and other adenine-based ligands with the ability to modulate the gating of native sheep cardiac RyR incorporated into planar phospholipid bilayers (Chan et al., 2000). With millimolar luminal [Ca^{2+}] and a maintained cytosolic [Ca^{2+}] of 10 μM, ATP induced P_o levels of approximately 0.9. The maximum P_o levels produced by the other adenine-based ligands investigated (ADP, AMP, adenosine, adenine) were much lower. CoMFA demonstrated a high correlation between ligand structure and maximum P_o induced. Although it is now well established that the purine ring is important for agonist activity (Morii and Tonomura, 1983; Meissner, 1984; Chan et al., 2000), we demonstrated that the phosphate groups are essential to the high efficacy of ATP. Our model predicts that the charge produced by the phosphate groups is the single most important factor that enables bound ATP molecules to activate the cardiac RyR channel to a greater extent than ligands with fewer phosphate groups (for example, ADP and AMP). To investigate the significance of the charge on the phosphate groups of ATP, we examined how reducing charge in this region would affect the gating of RyR channels. AMP-PCP is a nonhydrolysable analog of ATP in which a methyl group substitutes for the oxygen between the β- and γ-phosphate groups. The methyl substitution leads to a decrease in negative charge around the phosphate groups. We would predict a diminished ability of such a ligand to fully open the channel in the presence of 10 μM cytosolic Ca^{2+}. This pre-

This work was supported by the British Heart Foundation, National Science Foundation grant MCB9874761, and the University of Nevada Experiment Station.

ABBREVIATIONS: RyR, ryanodine receptor; CoMFA, comparative molecular field; CoMSIA, comparative similarity index analysis; AMP-PCP, adenosine-5′-(β,γ-methylenetriphosphate); SR, sarcoplasmic reticulum; EMD 41000, 2-(2-methoxy-4-methyl sulfonylphenyl)-3a,4,5,6,7,7a-hexahydro-1H-imidazo[4,5-*c*]pyridine.

diction, however, runs counter to accepted ideas about the effectiveness of AMP-PCP as an activator of RyR channels in that it is reported to be at least as effective as ATP (Smith et al., 1985). In fact, the stable nature of AMP-PCP has led to the routine use of this analog as a replacement for ATP in functional studies of RyR (for example, see Xu et al., 1996; Fruen et al., 2002).

Our single-channel experiments show that AMP-PCP is, as predicted from our initial model, a partial agonist at the ATP sites on the cardiac RyR, thus confirming the validity of our model. Importantly, we also show that AMP-PCP has a higher affinity for RyR than ATP, demonstrating that the affinity and efficacy of ligands at the ATP sites on RyR are dependent on different structural characteristics. Using the new information obtained from observing the effects of AMP-PCP on channel gating, we now present a more detailed description of the correlations between adenine nucleotide structure and the ability to open (efficacy) the sheep cardiac RyR channel. For the first time, we describe the structural characteristics of adenine nucleotides that are associated with high affinity for the ATP sites on the cardiac RyR. Electrostatic interactions are critically involved in the process of nucleotide binding to RyR, although steric factors also play a role. Use of comparative similarity index analysis (CoMSIA) demonstrates that although changes in hydrogen-bond acceptor ability of the adenine nucleotides are strongly correlated with changes in affinity of the ligand for RyR, it does not seem to influence the subsequent ability of the ligand to increase P_o.

Materials and Methods

Preparation of SR Membrane Vesicles and Planar Lipid Bilayer Methods. Heavy SR membrane vesicles were prepared from sheep hearts as described previously (Sitsapesan et al., 1991) and rapidly frozen and stored in liquid nitrogen. Vesicles were fused with planar phosphatidylethanolamine lipid bilayers as described previously (Sitsapesan et al., 1991). The vesicles were fused in a fixed orientation such that the *cis* chamber corresponded to the cytosolic space and the *trans* chamber to the SR lumen. The *trans* chamber was held at ground and the *cis* chamber held at potentials relative to ground. After fusion, the *cis* chamber was perfused with 250 mM HEPES, 125 mM Tris, and 10 μM free Ca^{2+} buffered with EGTA and $CaCl_2$, pH 7.2. The *trans* chamber was perfused with 250 mM glutamic acid and 10 mM HEPES and the pH was brought to 7.2 with $Ca(OH)_2$ (free $[Ca^{2+}]$, ~50 mM). Experiments were performed at room temperature (22 ± 2°C). The free $[Ca^{2+}]$ and pH of the solutions were determined at 22°C using a calcium plastic membrane half-cell (93-20; Thermo Orion, Beverly, MA) and epoxy body ROSS combination pH electrode (81-55; Thermo Orion) as described previously (Sitsapesan et al., 1991). Additions of ATP and AMP-PCP were made to the *cis* chamber and the free $[Ca^{2+}]$ was maintained at 10 μM at all ligand concentrations throughout all experiments.

Data Acquisition and Analysis. Single channel recordings were displayed on an oscilloscope and recorded on digital audio tape. Steady-state recordings were carried out at 0 mV. At this holding potential, Ca^{2+} current flows in the lumen-to-cytosol direction. The current recordings were filtered at 0.5 kHz (−3 dB) and digitized at 2 kHz using Satori (Intracel, Cambridge). Channel open probability (P_o) and the lifetimes of the open and closed events were determined over 3 min of recording using the method of 50% threshold analysis (Colquhoun and Sigworth, 1983). When more than one channel was incorporated into the bilayer, average P_o was calculated according to the formula: Average $P_o = [T_{open1} + 2(T_{open2}) + 3(T_{open3}). \ldots + N(T_{open\ n})]/NT_{total}$ where T_{open1}, T_{open2}, and T_{open3} are the times in the first, second, and third open channel levels, respectively, T_{total} is the total recording time, and N is the number of channels in the bilayer. The number of channels in the bilayer was determined by adding EMD 41000 (a caffeine analog that maximally activates the channels) at the end of each experiment. Lifetime analysis was carried out only when a single channel incorporated into the bilayer. Events <1 ms in duration were not fully resolved and were excluded from lifetime analysis. Lifetimes accumulated from 3-min steady-state recordings were stored in sequential files and displayed in noncumulative histograms. Individual lifetimes were fitted to a probability density function by the method of maximum likelihood (Colquhoun and Sigworth, 1983) according to the equation: $f(t) = a_1(1/\tau_1)\exp(-t/\tau_1) + \ldots + a_n(1/\tau_n)\exp(-t/\tau_n)$ with areas a and time constants τ. A missed-events correction was applied as described by Colquhoun and Sigworth (1983). A likelihood ratio test (Blatz and Magleby, 1986) was used to compare fits to up to four exponentials by testing twice the difference in $\log_e$ (likelihood) against the χ^2 distribution at the 1% level. Single-channel current amplitudes were measured from digitized data using manually controlled cursors. All P_o values are quoted as mean ± S.E.M., where $n \geq 4$. For $n = 3$, S.D. is given. The AMP-PCP dependence on P_o was characterized using the equation: $P_o = P_{max}(1/(1 + EC_{50}/[\text{AMP-PCP}]^{nH1}))\ (1 - (1 + (IC_{50}/[\text{AMP-PCP}])^{nH2}))$ where P_{max} equals the maximum P_o attained, EC_{50} and IC_{50} equal the half-maximum concentrations required for activation and inhibition, respectively, and n_{H1} and n_{H2} are the Hill coefficients of activation and inhibition, respectively.

CoMFA. A CoMFA is a mathematical expression of the correlation between the chemical structure of a collection of compounds and the experimentally determined biological activities of these compounds. (Cramer et al., 1988). Briefly, the Lennard-Jones (steric) potentials and electrostatic potentials are measured at the points in a three-dimensional array around each member of a series of compounds. Changes in these potentials are correlated with changes in the biological properties of the molecules using the method of partial least squares. We used SYBYL 6.6 (Tripos Associates, St. Louis, MO) and the Tripos force field for all of the calculations reported in this communication. The structures of ATP and analogs were correlated with the ability of these molecules to maximally activate the sheep cardiac RyR in the presence of 10 μM cytosolic Ca^{2+} and with the EC_{50} values for each compound. Briefly, the conformation of ATP was determined by extended molecular dynamics of ATP in adenylate kinase (Protein Data Bank Accession code, 1AKY (Abele and Schulz, 1995)). The alignments of the chemical structures are slightly changed from the previous report. The other compounds were built on the ATP framework and aligned to ATP by rigid-body field fitting. Cross-validation was used to test for predictive ability of the model. A cross-validated correlation coefficient of 1.0 indicates no deviation between predicted and measured biological properties; a value of 0.0 indicates a random correlation between structure and biological activity. A cross-validated correlation coefficient of 0.3 indicates a probability of less than 5% that the relationship between structure and activity is attributable to chance (Clark et al., 1990; Clark and Cramer, 1993). If the cross-validated correlation coefficients are sufficiently high, partial least-squares is used to build a model using all of the tested compounds. This final correlation coefficient can be interpreted analogously to a conventional correlation coefficient.

CoMSIA. CoMSIA, like CoMFA, is a mathematical expression correlating the chemical structures and biological activities of a set of compounds (Klebe, 1998). In CoMSIA, changes in physicochemical properties, such as hydrophobicity or hydrogen bond potential, can be compared with changes in biological activity.

Materials. ATP, adenosine, and adenine were 99% pure (Sigma, Poole, UK). EMD 41000 was a gift from Merck (64271 Darmstadt, Germany). Solutions were prepared using MilliQ de-ionized water (Millipore, Harrow, UK) and filtered through a Millipore membrane filter (pore size, 0.45 μm) before use. Other chemicals were AnalaR or the best equivalent grade from BDH or Sigma (Poole, UK).

Results

The Effects of AMP-PCP on RyR Channel Gating. Figure 1 illustrates how AMP-PCP activates single sheep cardiac RyR channels incorporated into planar lipid bilayers. RyR channel openings are typically brief when activated solely by 10 μM cytosolic Ca^{2+} as demonstrated in the top trace. AMP-PCP caused a dose-dependent increase in P_o, but even the most effective concentrations (500 μM–2 mM) could not fully activate the channels. Inspection of the traces shows that AMP-PCP produced large increases in the frequency of channel opening. At the maximum level of activation (illustrated in Fig. 1 and occurring at approximately 1 mM AMP-PCP), very brief open and closed events occurred, giving rise to a flickery appearance of gating. This flickery type of gating is characteristic of agents that activate the channel via the ATP sites (Kermode et al., 1998). ATP, itself, also causes flickery gating but at the most effective concentrations produces long events in addition to bursts of short open and closed events. Equivalent long open events were not observed with AMP-PCP under the controlled cytosolic [Ca^{2+}] and pH of the experiments. Figure 2 illustrates the typical gating behavior of a sheep cardiac RyR channel activated by 1 mM ATP. Consecutive single-channel recordings demonstrate the spontaneous changes in gating from high P_o levels characterized by long open times to lower P_o levels characterized by brief open and closed events. Over 3 min of recording, P_o averaged 0.89. This is approximately double the average maximum P_o obtained with AMP-PCP under the same experimental conditions (see Fig. 1). No measurable change in single-channel conductance was observed after addition of AMP-PCP to the cytosolic chamber (results not shown).

The relationship between P_o and [AMP-PCP] is shown in Fig. 3. The maximum P_o obtained was 0.441 ± 0.156 at 1 mM AMP-PCP (SEM; $n = 4$), well below the maximum P_o level that could be achieved with ATP (~0.9) under identical experimental conditions. The results highlight the partial agonist nature of AMP-PCP. The EC_{50} value for channel activation by AMP-PCP was 164 μM. This is lower than the EC_{50} for channel activation by ATP which is 220 μM (Kermode et al., 1998) indicating that AMP-PCP has a higher affinity for the cardiac RyR than ATP. The Hill coefficient for channel activation by AMP-PCP was 2.1 indicating that multiple AMP-PCP molecules must bind to the channel to produce the maximum effect. Concentrations of AMP-PCP above the optimum doses produced channel inactivation, as observed for other adenine nucleotides (Kermode et al., 1998; Ching et al., 1999).

The modulation of P_o by AMP-PCP resulted from changes in both the open and closed lifetime durations. Channel activation was caused mainly by dose-dependent reductions in the mean closed times. For example, in a typical channel activated by 10 μM cytosolic Ca^{2+}, 500 μM AMP-PCP reduced the mean closed time from 101 to 1.63 ms, whereas the mean open time was increased only from 0.51 to 2.62 ms. High [AMP-PCP], which produced channel inactivation re-

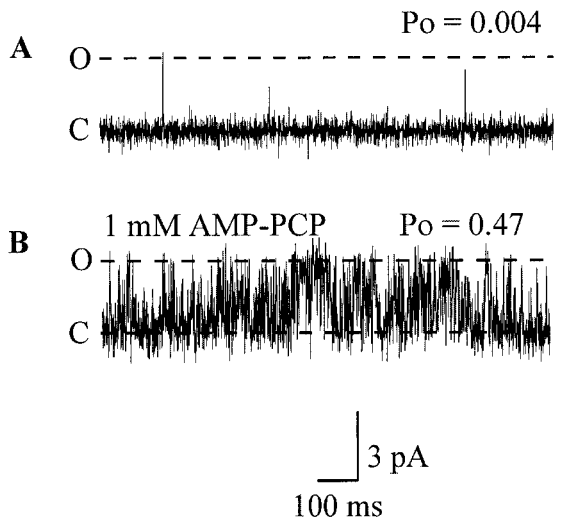

Fig. 1. Effects of AMP-PCP on current fluctuations through a typical single sheep cardiac RyR. A, the channel is activated by 10 μM cytosolic Ca^{2+}. B, 1 mM AMP-PCP has been added to the *cis* chamber. The free cytosolic [Ca^{2+}] is maintained at 10 μM. O and C indicate the open and closed channel levels, respectively. The figure illustrates an optimal concentration of AMP-PCP under these experimental conditions.

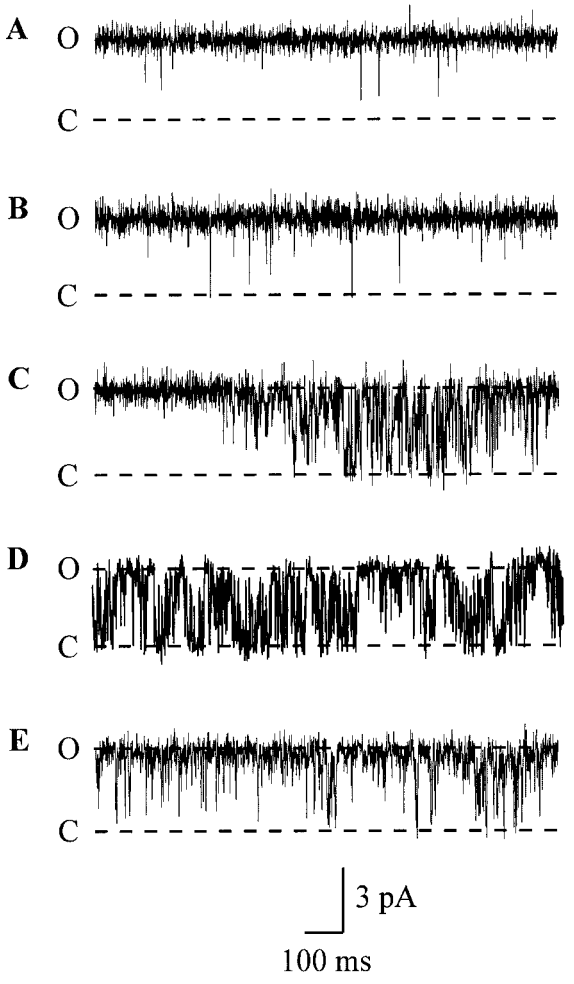

Fig. 2. Effects of ATP on RyR channel gating. The variation in gating observed over time in a typical single cardiac RyR channel activated by 10 μM cytosolic Ca^{2+} alone and 1 mM ATP (in the presence of 10 μM free cytosolic Ca^{2+}) is shown. Sequential single-channel recordings of the channel are shown. Measurement of P_o over 3 min of continuous recording gives an average P_o of 0.89. ATP elicits long open events, as shown in traces A and B, but the channel can also revert to flickery gating characterized by brief opening and closing events as shown in traces C and D. In trace E, some flickery gating can be observed interspersed with longer open events. O and C indicate the open and closed channel levels, respectively.

versed the changes in mean open and closed time durations: 2 mM AMP-PCP produced an increase in the mean closed time to 7.31 ms and a decrease in mean open time to 0.8 ms.

How Does AMP-PCP Activation of RyR Compare with the Effects of Other Adenine Nucleotides? In Fig. 4, we compare the affinity, efficacy, and Hill coefficient for the activation of the cardiac RyR by AMP-PCP and other adenine nucleotides (Chan et al., 2000). The properties of AMP seem to deviate significantly from those of the other ligands shown. AMP has a very low affinity for RyR, a low ability to increase P_o, and also activates the channel with a Hill coefficient <1. ADP, although it has a low affinity and shows no evidence for a positively co-operative action, still has a greater ability to open the channel if present in sufficient quantities (≥10 mM). In the presence of 10 μM cytosolic Ca^{2+}, AMP-PCP is not able to produce the same high level of activation as ATP because it does not induce long enough open events. AMP-PCP, however, has the highest affinity for RyR and the highest Hill coefficient of all the adenine nucleotides studied.

CoMFA of P_o. The CoMFA values of P_o described in this article are similar to those obtained earlier with the more limited data set (Chan et al., 2000). In the previous report, electrostatic factors accounted for 64% of the observed correlation between structure and P_o. Steric factors accounted for the remaining 36%. In this report, we have used P_o to calculate the increased free energy required to raise the P_o above that seen in the presence of Ca^{2+} and zero ATP analog. This is calculated as $\Delta\Delta G = (1.987 \text{ cal/mol K})(296 \text{ K})[\ln((P_o \text{ in the presence of ATP analog})/(P_o \text{ in the presence of } Ca^{2+} \text{ only}))$. The bilayer experiments were done at 23°C (296 K). The cross-validated correlation coefficient (a measure of predictive ability) for P_o is 0.307 with a final correlation coefficient (r^2) of 0.994.

Interestingly, AMP is the greatest outlier, not AMP-PCP. The model seems reliable for analysis of the relationship between structure and activity of this group of compounds because of A) the extreme stability of the model in bootstrapping (extremely low S.E.E., < 0.1%, data not shown), B) the linearity of the correlation between predicted and experimental values (r^2); and C) the close agreement between predicted and experimental values (9% error or less). Omission of AMP-PCP from the data set increases the cross-validated correlation coefficient to 0.558 (final correlation coefficient, 0.998). In CoMFA, the correlation between structure and activity is based on the steric and electrostatic properties of the compounds. If a correlation exists, as in this case, the CoMFA can assign how much of the structure-activity relationship can be explained by steric or electrostatic differences between the compounds. For the groups of compounds re-

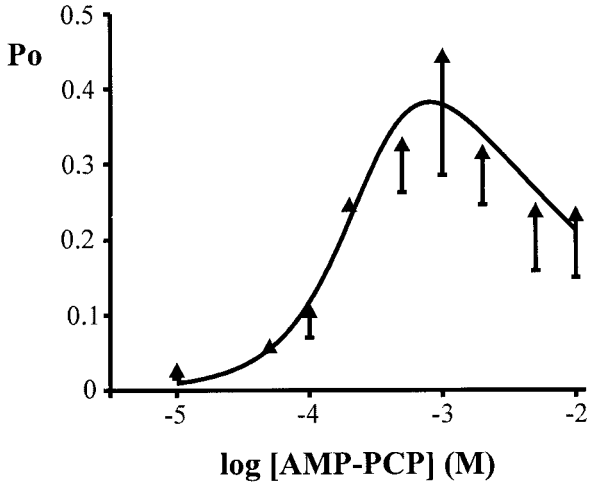

Fig. 3. Relationship between P_o and AMP-PCP concentration in the presence of 10 μM free cytosolic Ca^{2+}. S.E.M. for $n \geq 4$ is shown.

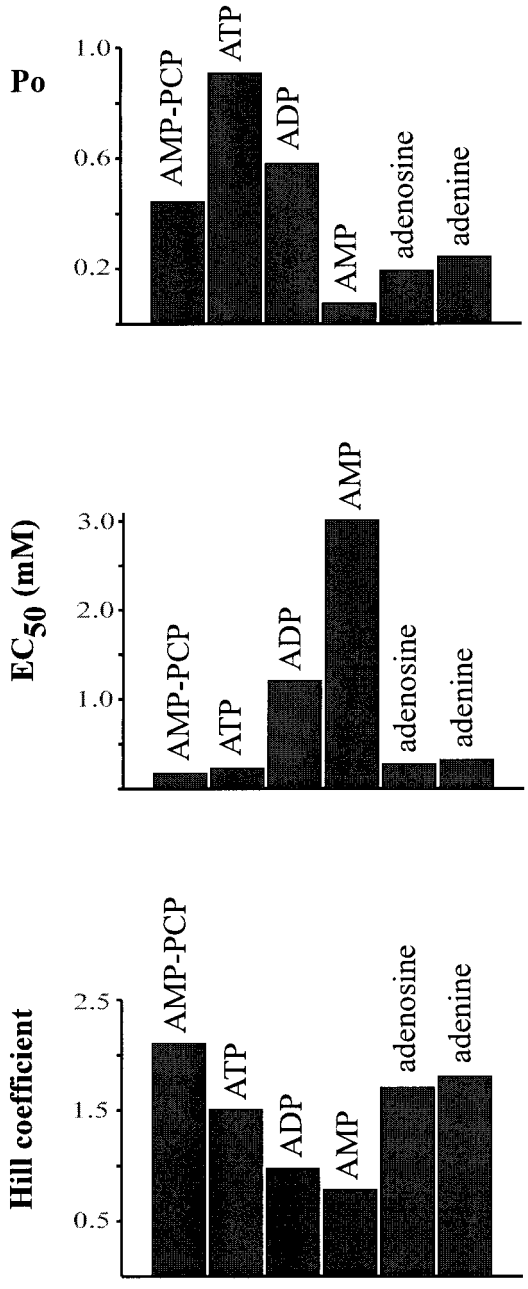

Fig. 4. Comparison of the actions of AMP-PCP with ATP, ADP, AMP, adenosine, and adenine on cardiac RyR channel gating in the presence of 10 μM free cytosolic Ca^{2+}. Top, maximum P_o that can be achieved with each ligand. Center, comparison of EC_{50} values. Bottom, Hill coefficient for RyR channel activation for each ligand. The dose ranges used to obtain the above information were: AMP-PCP, 10 μM–10 mM; ATP, 10 μM–20 mM; ADP, 100 μM–50 mM; AMP, 100 μM–10 mM; adenosine, 10 μM–5 mM; adenine, 20 μM–5 mM. For AMP-PCP, ATP, ADP, AMP, adenosine, and adenine, maximum P_o was observed at 1, 2, 20, 20, 1, and 2 mM, respectively.

ported here, 69% of the correlation is attributable to differences in electrostatic fields of the compounds and 31% is attributable to differences in the steric (van der Waals) properties of the compounds. Electrostatic factors dominate steric factors. In the previous report, we contoured the relationship between changes in the steric and electrostatic fields at the nucleotide binding site and the ability of the adenine nucleotides to increase P_o. In Fig. 5, we show a similar diagram illustrating the relationships between changes in structure and changes in the maximum P_o attainable after inclusion of AMP-PCP into the data set. Such diagrams are useful in visualizing how physicochemical factors modulate channel function.

An important property of a CoMFA is the ability to predict the properties of novel compounds. The CoMFA presented earlier (Chan et al., 2000) predicted the free energy of the missing AMP-PCP well. It correctly predicted that AMP-PCP would be less effective than ATP in promoting P_o. For comparison, the experimental P_o of ATP is 0.90, the predicted P_o of AMP-PCP is 0.78, and the experimentally determined P_o of AMP-PCP is 0.44. The predicted value of AMP-PCP is a reasonable extrapolation of the CoMFA from the oxygen bridging the terminal phosphorus atoms in ATP to the carbon bridge in AMP-PCP. The error of the estimate is 909 cal/mol compared with the experimentally determined free energy change of 1993 cal/mol (a 46% error). When AMP-PCP is included in the CoMFA basis set, the error decreases to 24 cal/mol (a 1% error). Unless otherwise noted, the full basis set (including AMP-PCP) will be used for all following analyses.

CoMSIA of P_o. Using CoMSIA, no correlations were found between changes in steric bulk, hydrogen bonding, or hydrophobicity and the ability to modulate P_o. None of these properties, when tested alone, was sufficient to explain the differences in biological activities. The lack of correlation was seen regardless of inclusion of AMP-PCP in the test group of compounds. Only electrostatic CoMSIA showed strong correlations between changes in structure and changes in P_o (q^2 = 0.624, r^2 = 0.992). Of the properties tested, only the electrostatic field is sufficient by itself to predict P_o.

CoMFA of EC_{50}. We have expressed EC_{50} values as the apparent free energy of binding. This is calculated as ΔG = (1.987 cal/mol K)(296 K)[ln (EC_{50})]. The cross-validated correlation coefficient (q^2) for EC_{50} is 0.583 (r^2 = 1.00). As for P_o, most of the correlation (66%) is between changes in electrostatic field and changes in EC_{50}. The remainder of the correlation is with changes in steric bulk. Figure 6 illustrates the locations in which changes in structure are most highly correlated with changes in EC_{50}, and compares the regions in which steric and electrostatic factors play the greatest role.

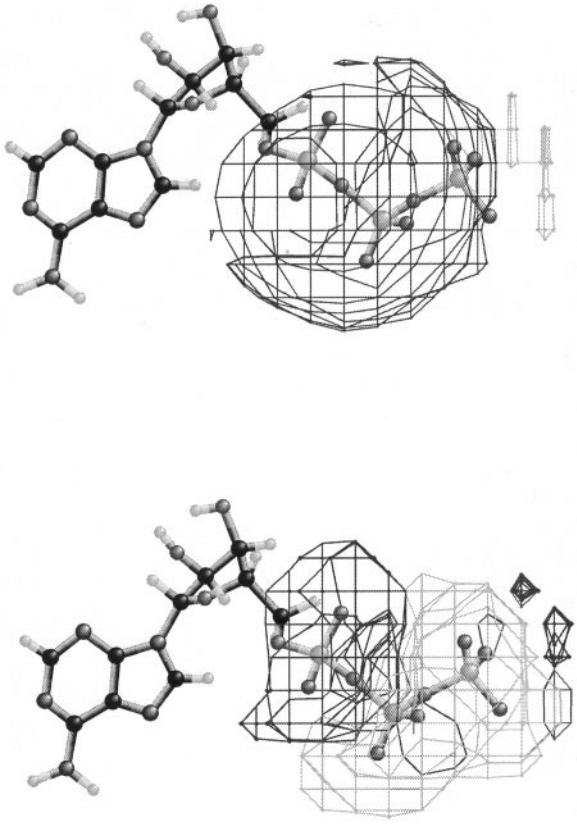

Fig. 5. CoMFA of P_o. The wire frames show the regions in space where changes in structure are most strongly correlated with changes in P_o. A ball-and-stick representation of ATP is shown as a guide to the eye. Top, gray contours illustrate the regions where increased negative charge is correlated with increased P_o; black contours illustrate the regions where increased positive charge is correlated with increased P_o. The black contours reflect the increasing P_o because the highly charged terminal phosphate is located further from the adenyl group. Bottom, gray contours detail where increased steric bulk is correlated with increased P_o, and black contours show where increased steric bulk is correlated with decreased P_o

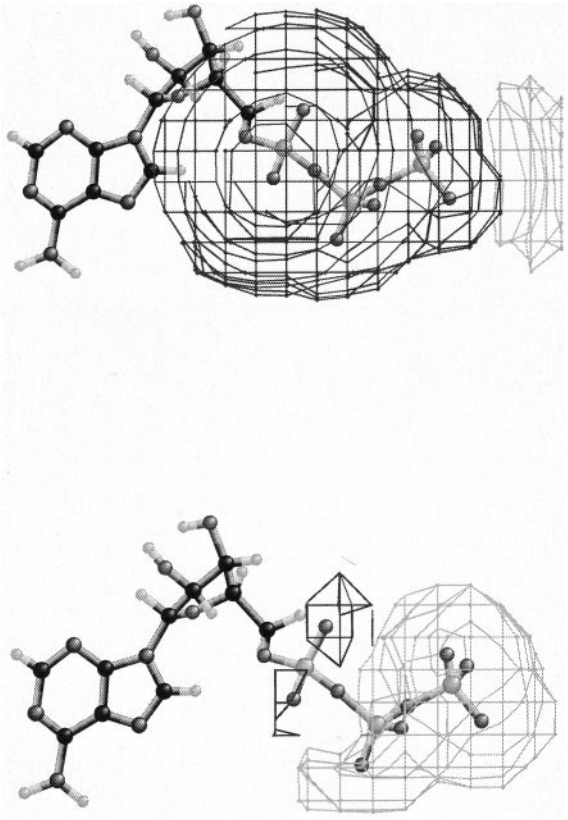

Fig. 6. CoMFA of EC_{50}. Regions in space where changes in structure are most strongly correlated with changes in affinity are shown. Top, gray contours illustrate the regions where increased negative charge is correlated with a decrease in EC_{50}, and black contours show the regions where increased positive charge is correlated with decreased EC_{50}. Bottom, gray contours detail where increased steric bulk is correlated with a decrease in EC_{50}, and black contours show where increased steric bulk is correlated with increased EC_{50}.

CoMSIA of EC_{50}. In contrast to the correlation with P_o, additional analysis by CoMSIA found a correlation between hydrogen-bond acceptor ability and changes in EC_{50} (cross-validated correlation coefficient, 0.330; final correlation coefficient, 1.0). Figure 7 details the regions in which hydrogen-bond accepting properties are correlated most strongly with the affinity of the adenine nucleotides for RyR. As was the case with P_o, a correlation was seen with changes in electrostatic CoMSIA but not hydrogen-bond donating, hydrophobic potential, or steric bulk. The results demonstrate that at least part of the difference between the ligand-receptor interactions leading to changes in P_o and EC_{50} is the importance of hydrogen-bond accepting ability of the modulators.

Structure-Activity Relationships and Energetic Considerations. By correlating the single-channel effects of ATP and related ligands with their structural characteristics, we can distinguish between the structural properties required to produce strong binding to RyR and those required to drive the channel into the open state. Interactions between a ligand and a receptor can be divided into two broad types: A) those that exist in the ligand-receptor complex only and B) those that relate the relative solvation of the ligand by the receptor to that of the bulk medium (including counter ions, detergents, and so forth). In this report, the properties of AMP-PCP as an agonist at ATP sites on RyR have been analyzed in the context of other nucleotides and analogs. The properties compared include the maximum P_o, the concentration of ligand required to produce half-maximum P_o (EC_{50}), the Hill coefficient, and the mean open and closed lifetimes. Of these, the P_o and any altered open and closed life times are properties of the ligand-receptor complex only. These quantities are often obtained at saturating levels of ligand (e.g., P_o). They depend not on affinity of ligand for the binding site but on complementary interactions in the ligand-receptor complex that can provide energy to alter the equilibrium between open and closed states or to lower the energy barrier between open and closed states. In the following analysis, the focus will be on the energetic relationships measured by P_o and EC_{50}.

Ultimately, the energy to modulate the channel comes from the binding energy. To the extent that binding energy will be used to favor channel opening, alter the state of allosteric sites, or lower transition state energies, the apparent binding energies will be lessened. For every calorie used to push the channel to the open state, one less calorie will be available to increase the affinity constant. These relationships will be reflected in the EC_{50} of the various effectors. Therefore, correlations between EC_{50} and structure reflect both the intrinsic affinity of receptor for ligand and the conversion of binding energy into conformational energy (e.g., the total energy of binding less the energy required to increase P_o).

One can gain a quantitative insight into the structural features of ATP that produce the experimentally observed P_o and EC_{50} by creating imaginary molecules and using the CoMFA to predict the P_o and EC_{50}. This type of analysis has been used to predict the effects of the imaginary compounds listed in Table 1. In Table 2, the calculated free energy of binding and free energy used to increase P_o are shown for the different ligands. A comparison of the percentage of the total energy used by each ligand to activate RyR is shown.

Distribution of Energies Responsible for ATP Modulation of P_o and EC_{50}. Addition of ligands such as ATP increases the value of P_o above that seen with Ca^{2+} alone. This difference in P_o can be related to the additional free energy ($\Delta\Delta G$) required to push the equilibrium toward the open states of the RyR. In the case of ATP, the shift in P_o requires the input of 3459 cal/mol of free energy (Table 1). We used CoMFA to show quantitatively the distribution of this energy among the components of the most effective ligand, ATP. To do this, we have created imaginary molecules by removing fragments of the ATP and used CoMFA to predict the properties of these constructs. In the first column of Table 1, the missing elements are indicated by a space. The indicated fragments of the molecule remaining are left with the same charge and atomic positions as the intact ATP. In columns 2 and 3, we have calculated the free energies of these virtual molecules.

From Tables 1 and 2, it is apparent that the β and γ phosphates contribute most of the interactions that drive the RyR to an open state. In this regard, it is interesting to note that the predicted value of row two (Table 1) (an imaginary compound equivalent to ADP) has a predicted free energy of

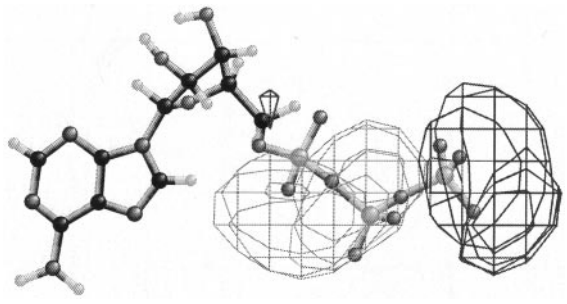

Fig. 7. CoMSIA of hydrogen bond acceptor ability and EC_{50}. The wire frames show the regions in space where changes in structure are most strongly correlated with changes in hydrogen bond acceptor ability. Hydrogen bond acceptor potential is itself sufficient to make a reasonably reliable prediction of the EC_{50} of the compounds tested. The black wire frames are those areas in which increasing hydrogen bond accepting potential is highly correlated with decreasing EC_{50}. The gray wire frames are those areas in which increasing hydrogen bond accepting potential is highly associated with increasing EC_{50}. The position of the contours reflects the decrease in EC_{50} as hydrogen bond acceptors are moved outward from the nucleoside.

TABLE 1

Anatomy of the ATP-RyR interaction: distribution energy calculated from the experimental EC_{50} and the maximum increase in P_o

The imaginary compounds are indicated by the missing parts of the linear formula. The first row is the complete ATP molecule. Row two contains an imaginary molecule obtained by omitting the terminal (γ) PO_3; the atoms remaining have exactly the same position and charge as in ATP. Row 2 is similar, but not identical to, the ADP used in the experimental data. Row 3 is obtained from ATP (row 1) by removal of the β PO_2 group. This is similar (but not identical) to an AMP plus a phosphate. In row 4, the α PO_2 group is removed. This is similar to an adenosine plus a pyrophosphate. In row 5, the ribose is omitted. In row 6, the adenine base is omitted. The values in columns 2 and 3 are calculated with the indicated atoms missing while the remaining atoms retain the charge, position, and other properties found in ATP. The experimentally determined values are shown in parentheses for comparison with the predicted values of ATP.

Compound	ΔG	
	P_o	EC_{50}
	cal/mol	
Adenine-ribose-O-P-O-P-O-P-O	3451 (3459)	4952 (4956)
Adenine-ribose-O-P-O-P-O	2115	3952
Adenine-ribose-O-P-O O-P-O	2399	4629
Adenine-ribose-O O-P-O-P-O	3226	5179
Adenine O-P-O-P-O-P-O	3869	4879
ribose-O-P-O-P-O-P-O	3352	4988

2115 cal/mol compared with the experimentally determined value for ADP of 2318 cal/mol (Table 2, column 2). The imaginary ADP-like fragment is much less effective than ATP in promoting the open state of the channel (only providing 61% of the free energy of ATP, in agreement with the experiment). One might surmise that ADP + P_i would be more effective than ADP alone. However, we have found that addition of P_i to ADP does not enhance ryanodine binding above that seen in the presence of ADP alone (W. M. Chan, W. Welch, R. Sitsapesan, manuscript in preparation). Therefore, the P_i does not simply play a passive role (e.g., to neutralize a charge on the receptor to allow a higher P_o). The physical relationship between the γ-phosphate and the remainder of the nucleotide is important: they form a device to coerce the RyR into a conformation with a high value of P_o. In the context of ATP, the adenyl fragment contributes only a small part of the energy driving the increase in P_o ([predicted value for ATP] − [predicted value for ribose triphosphate] = 99 cal/mol) and contributes essentially nothing to binding (EC_{50}). According to this prediction, at saturation, a ribose triphosphate should be nearly as effective as ATP in promoting high P_o. It would be interesting to conduct this experiment to determine the importance of the nucleotide base in the determination of P_o and EC_{50}.

These predictions are of interest because of the relationship with the experimental data. First, although the base contributes little in the context of ATP, the RyR is specific for the base. The ATP analog GTP is incapable of increasing P_o, even at concentrations well beyond those that fully saturate the ATP effect. Second, adenine alone can promote P_o by 1287 cal/mol (Table 2, column 2) and has apparent free energy of binding (obtained from the EC_{50} value) of 4523 cal/mol (Table 2, column 3). The result is not a fluke of the CoMFA. The predicted contribution of an imaginary adenyl fragment [formed by removing all atoms from ATP except those of the adenyl group (i.e., the negative of row 6 of Table 1)] was calculated. The predicted free energy to increase P_o is 1464 cal/mol, near the experimentally determined value for adenine (1287 cal/mol; Table 2, column 2). Likewise, the predicted free energy of binding (from EC_{50}) is 4447 cal/mol, near the experimentally determined value of 4523 cal/mol (Table 2, column 3). Therefore, the interactions between receptor and ligand are complex and depend upon the context in which the components of the ligand are presented to the receptor, including any ligand-induced changes in receptor conformation. If the charges are removed from ATP (i.e., the charge on all atoms is set to zero, all other atomic properties remain), the predicted energy drops from 3451 cal/mol to 1151 cal/mol. The latter number reflects the steric contribution to the enhanced P_o.

TABLE 2

Comparison of free energy of binding to free energy used to increase P_o

The free energies were calculated from the experimentally observed increase in P_o (ΔΔG column) or from the experimentally measured EC_{50} for increased P_o (ΔG column). See the text for the formulae used. The total binding energy is estimated by summing the ΔΔG and ΔG columns. This calculation neglects the contribution of binding energy to lowering transition state energies and interaction energies manifested in the Hill coefficient. The percentage of binding energy converted to increasing the P_o is estimated by dividing the value in the ΔΔG column by the value in the ΔG(total) column and multiplying by 100.

Compound	ΔΔG (P_o)	ΔG (EC_{50})	ΔG (total)	Modulation
				%
ATP	3459	4956	8415	41
ADP	2318	3958	6276	37
AMP	619	3419	4038	15
Adenosine	1035	4619	5654	18
Adenine	1287	4523	5810	22
AMPPCP	1993	5129	7122	28

Conversion of Binding Energy to Modulation Energy. The total binding energy of ATP (Table 2, column 4; 8415 cal/mol) can be estimated from the sum of the experimental energies from the EC_{50} (4956 cal/mol) and the incremental increase in the P_o (3459 cal/mol, see Table 2). Forty percent of the total binding energy is used to modulate channel function. In the case of ADP, the total binding energy is 6276 cal/mol as estimated from the sum of the experimental energies from the EC_{50} (3958 cal/mol) and the incremental increase in P_o (2318 cal/mol). Again, about 40% of the binding energy is used to increase the open probability of the channel. Therefore, the difference between the P_o induced by ATP and ADP seems to be caused by the difference in total energy available.

In contrast, the total binding energy of adenine is 5810 cal/mol (4523 cal/mol from EC_{50} and 1287 cal/mol from the incremental increase in P_o). Only 22% of this smaller binding energy is converted to modulation of the channel. Interestingly, the total binding energy of the larger molecule adenosine (5654 cal/mol, 4619 cal/mol from EC_{50} and 1035 cal/mol from P_o) is slightly lower than that of adenine. This reflects the antagonism that the sugar ring exerts on channel modulation (see Table 1). Similarly to adenine, 18% of the total binding energy is diverted to modulate the channel P_o. In summary, the base and sugar provide binding energy and position the β- and γ-phosphates to promote channel opening.

Interaction Energy. As stated previously, the energy to modulate P_o and mean open and closed times comes from the energy of nucleotide-receptor interactions. Unfortunately, at this time, no atomic level model of the nucleotide-binding site of the RyR exists. However, nucleotide-binding sites are generally considered to have a common structural motif. To investigate the effects of nucleotide analog structure on ligand-receptor interactions, we used molecular dynamics to estimate changes in interaction energy using adenylate kinase (Protein Data Base code 1AKY) as a surrogate for the nucleotide-binding site on the RyR. The interaction energy of ADP is 80% of that of ATP (molecular dynamics data not shown). This value compares well with those in the paragraph above. The incremental increase in P_o induced by ADP (2318 cal/mol) is 67% of that of ATP (Table 2, column 2). The total binding energy of ADP (6276 cal/mol) is 74% of that of ATP (Table 2, column 4). The binding energy of ADP estimated from the EC_{50} value (3958 cal/mol) is 80% of that of ATP (Table 2, column 3). In the present study, therefore, a surrogate nucleotide-binding site reasonably parallels the experimentally observed nucleotide-RyR interactions.

Discussion

Our preliminary CoMFA model (Chan et al., 2000) predicted that, in the presence of 10 μM cytosolic Ca^{2+}, AMP-PCP would be significantly less effective than ATP as an activator of the cardiac RyR channel. Our results demonstrated that the maximum P_o achieved by AMP-PCP was approximately half that obtained with ATP (Figs. 1 and 3). Although these results provided conformation of the validity of our model, they were still surprising in light of previous

reports of the effectiveness of AMP-PCP to activate RyR channels. The literature contains no hint that AMP-PCP would lack efficacy, in fact quite the reverse. There are, however, a number of possible reasons to explain these discrepancies. First, in early reports, only a single dose of AMP-PCP had been compared with a single dose of ATP (Smith et al., 1985) and subsequent investigators did not examine the full dose-response relationship of these ligands. Second, because the effects of adenine nucleotides are strongly Ca^{2+}-dependent, slight differences in free $[Ca^{2+}]$ could lead to large changes in AMP-PCP–induced effects. Third, it is possible that AMP-PCP has a higher efficacy at the skeletal isoform of RyR than at the cardiac isoform. Finally, we have demonstrated in the present study that AMP-PCP has a higher affinity for the cardiac RyR than ATP. The relatively high affinity of AMP-PCP for RyR will have masked its low efficacy in studies such as [^{3}H]ryanodine binding studies or Ca^{2+} flux experiments. This type of experiment is often designed to produce the maximum possible measurable response; therefore, relatively low concentrations of a nucleotide can produce the maximum level of [^{3}H]ryanodine binding or the maximum increase in the rate of Ca^{2+} efflux from SR membrane vesicles. Thus, partial agonists and full agonists will induce the same maximum level of [^{3}H]ryanodine binding although a high-affinity ligand may seem to be more effective at opening RyR at low concentrations. It is impossible, therefore, to distinguish between the efficacy and affinity of a ligand under these conditions.

In this study, not only did we find that AMP-PCP has a higher affinity for the cardiac RyR than ATP, we also demonstrated that AMP-PCP activates the channel with a higher degree of positive cooperativity. The Hill coefficient for AMP-PCP was 2.1, whereas for ATP, the Hill coefficient was 1.5 (Kermode et al., 1998). An increase in cytosolic $[Ca^{2+}]$ produced a marked increase in the Hill slope for activation of the cardiac RyR by AMP (Ching et al., 1999). If this is true of adenine nucleotide channel activation in general, then the effects of AMP-PCP may be much more sensitive than ATP to changes in cytosolic $[Ca^{2+}]$ because of its apparently greater degree of positive cooperativity. These subtle differences in the characteristics of AMP-PCP and ATP may produce marked differences in RyR channel gating. Use of AMP-PCP as a nonhydrolysable "physiological replacement of ATP" may not, therefore, produce reliable results.

The structure-activity relationship reported here demonstrates that the interactions between ATP and related compounds are complex, consistent with a mechanism whereby at least part of the binding energy is converted into conformational changes in the receptor. Adenine triphosphate is the most effective ligand because, at least in part, it has the highest binding energy and because it converts the greatest percentage of its binding energy into increased P_o. Another interesting observation is the relationship of the nucleotide base with P_o, EC_{50} and ligand specificity. The data in Table 1 imply that, in the context of ATP, the base contributes an unimportant amount of energy to the increase in P_o or to binding (EC_{50}), yet the RyR is specific for the adenine fragment. Replacement of the adenine with a guanine completely destroys the ability of the nucleotide to modulate RyR. This fact suggests a tight complementarity at the base sub-binding site such that the additional steric bulk (and/or polar interaction) at the 2-positon of the base blocks nucleotide binding. In addition, the unligated adenine binds with reasonable strength and promotes a significant increase in P_o (Table 2). We suggest that interactions between adenine and receptor are weakened in the context of ATP because of binding-induced conformational changes in receptor, ligand, or both. To maximize interactions between receptor and the triphosphate, interactions between receptor and base are relaxed (but not to the point of loss of specificity). We suggest that the ligands bound to the nucleotide site do not serve a permissive role (for example, shielding unfavorable interactions); instead, they are active participants in the functional state of the RyR and different ligands induce or stabilize unique conformers of the RyR. The conformers are manifested not in the magnitude of the conductance but in the equilibrium between open and close channel states and the energy barrier between them. To make an analogy with enzyme-catalyzed reactions, the bound ligand may stabilize one or more transition states between conducting and nonconducting forms of the channel and the ligand may bind somewhat more tightly to the conducting form of the RyR.

Hill coefficients derived from the experimental data indicate that there may be more that one nucleotide binding site per RyR channel. Because RyR is a homotetramer, there may be four nucleotide binding sites per tetramer. However, the three-dimensional structure-activity relationships described in the present study are based on EC_{50} values and maximum P_o levels induced. The relationships are therefore not dependent upon assumptions about the number of binding sites or interactions between sites and cannot be used to explain any cooperativity observed. An important future investigation would be to examine the effect of nucleotide structure on the cooperativity of adenine-nucleotide–induced stimulation of P_o.

With increasing knowledge of the effects of adenine nucleotides on RyR gating, the more obvious the high efficacy of ATP becomes and the greater our certainty that the γ-phosphate group of ATP plays a unique role in allowing ATP to induce long open states and high P_o values. These results prompt the question of whether some of the effects of ATP could be caused by phosphorylation of the channel. Indeed, a recently published report suggests that part of the effects of ATP on the skeletal isoform of RyR results from phosphorylation of the channel by CaMKII (Dulhunty et al., 2001). However, we have no evidence that this is the case in our experiments. Unlike the report by Dulhunty et al. (2001), the effects of ATP that we observe are completely reversible; after 25–30 min in the presence of cytosolic ATP (1–5 mM), perfusion of the cytosolic chamber completely reverses the effects of ATP. Moreover, we have no evidence for any time-dependent increases in P_o, as would be expected to occur if phosphorylation of RyR were producing a change in gating. Compelling evidence that phosphorylation is not producing our ATP-dependent changes in gating comes from the CoMFA itself. Cross-validation of the molecules used in the CoMFA analysis demonstrates that ATP is not an outlier, as would be expected if some of the effects of ATP were caused by phosphorylation. We therefore have strong evidence that our reported effects of ATP on the gating of cardiac RyR channels are caused by ligand-receptor interactions that do not involve phosphorylation. Possibly, the differences between our results and those of Dulhunty et al. (2001) reflect differences in the effects of ATP on skeletal and cardiac

channels. Alternatively, the differences may be caused by variations in the preparation of the heavy SR membrane vesicles, which could alter the phosphorylation state of RyR or the attachment of associated proteins to RyR.

In this study, the effects of adenine nucleotides have been examined in the presence of only one other modulator of RyR channel activity, cytosolic Ca^{2+}, and the concentration of Ca^{2+} has been maintained at 10 μM so that the effects of the nucleotides rather than the effects of changes in [Ca^{2+}] can be monitored. During EC-coupling, the RyR will experience cyclical changes in cytosolic [Ca^{2+}] from 0.1 to >10 μM, so it is important that future studies investigate the ability of adenine nucleotides to modulate RyR activity at a range of cytosolic [Ca^{2+}]. Moreover, approximately 0.5 mM Mg^{2+} is present in cardiac cells and it not known how the effects of the Mg^{2+}-bound form of ATP differ from those of the Ca^{2+}-bound form. Future experiments must address this by comparing the actions of nucleotides in the presence and absence of physiological levels of Mg^{2+}, although this is complicated because Mg^{2+} itself also modulates RyR P_o directly.

In summary, we have demonstrated the reliability of our CoMFA model to predict the ability of ATP analogs to open the cardiac RyR channel. We also report on a new CoMFA model that describes the correlation between adenine nucleotide structure and affinity for RyR. The structural features responsible for high affinity differ from those responsible for high efficacy. The results of this study provide insight into the molecular mechanisms by which adenine nucleotides open the cardiac RyR and should provide a greater understanding of how adenine nucleotides regulate SR Ca^{2+} release in cardiac cells.

References

Abele U and Schulz GE (1995) High-resolution structures of adenylate kinase from yeast ligated with inhibitor Ap5A, showing the pathway of phosphoryl transfer. *Protein Sci* **4:**1262–1271.

Blatz AL and Magleby KL (1986) A quantitative description of 3 modes of activity of fast chloride channels from rat skeletal muscle. *J Physiol* **378:**141–174.

Chan WM, Welch W, and Sitsapesan R (2000) Structural factors that determine the ability of adenosine and related compounds to activate the cardiac ryanodine receptor. *Br J Pharmacol* **130:**1618–1626.

Ching LL, Williams AJ, and Sitsapesan R (1999) AMP is a partial agonist at the sheep cardiac ryanodine receptor. *Br J Pharmacol* **127:**161–171.

Clark M and Cramer IRD (1993) The probability of chance correlation using partial least squares (PLS). *Quant Struct-Act Relat* **12:**137–145.

Clark M, Cramer RD 3rd, Jones DM, Patterson DE, and Simeroth PE (1990) Comparative molecular field analysis (CoMFA): towards its use with 3D-structural databases. *Tetrahedron Comp Method* **3:**47–60.

Colquhoun D and Sigworth FJ (1983) Fitting and statistical analysis of single-channel recording, in *Single-Channel Recording* (Sakmann B and Neher E eds) pp 191–263, Plenum, New York & London.

Cramer RD 3rd, Patterson DE, and Bunce JD (1988) Comparative molecular field analysis (CoMFA). 1. Effect of shape on binding of steroids to carrier proteins. *J Am Chem Soc* **110:**5959–5967.

Dulhunty AF, Laver DR, Curtis SM, Pace S, Haarmann C, and Gallant EM (2001) Characteristics of irreversible ATP activation suggest that native skeletal ryanodine receptors can be phosphorylated via an endogenous CaMKII. *Biophys J* **81:**3240–3252.

Fruen BR, Bardy JM, Byrem TM, Strasburg GM, and Louis CF (2002) Differential Ca^{2+} sensitivity of skeletal and cardiac muscle ryanodine receptors in the presence of calmodulin (Abstract) *Am J Physiol* **279:**C724–C733.

Kermode H, Williams AJ, and Sitsapesan R (1998) The interactions of ATP, ADP and inorganic phosphate with the sheep cardiac ryanodine receptor. *Biophys J* **74:** 1296–1304.

Klebe G (1998) Comparative molecular similarity indices: CoMSIA, in *3D QSAR in Drug Design* (Kubinyi H, Folkers H, and Martin YC eds) pp 87–104, Kluwer Academic Publishers, London.

Meissner G (1984) Adenine nucleotide stimulation of Ca^{2+}-induced Ca^{2+} release in sarcoplasmic reticulum. *J Biol Chem* **259:**2365–2374.

Morii H and Tonomura Y (1983) Ca^{2+}-induced Ca^{2+} release from fragmented sarcoplasmic reticulum. *J Biochem* **93:**1271–1285.

Sitsapesan R, Montgomery RAP, MacLeod KT, and Williams AJ (1991) Sheep cardiac sarcoplasmic reticulum calcium release channels: modification of conductance and gating by temperature. *J Physiol* **434:**469–488.

Smith JS, Coronado R, and Meissner G (1985) Sarcoplasmic reticulum contains adenine nucleotide-activated calcium channels. *Nature (Lond)* **316:**446–449.

Xu L, Mann G, and Meissner G (1996) Regulation of cardiac ca^{2+} release channel (ryanodine receptor) by Ca^{2+}, H^+, Mg^{2+}, and adenine nucleotides under normal and simulated ischemic conditions. *Circ Res* **79:**1100–1109.

Address correspondence to: Dr. R. Sitsapesan, University of Bristol, Department of Pharmacology, School of Medical Sciences, University Walk, Bristol BS8 1TD, UK. E-mail: r.sitsapesan@bris.ac.uk